Available online at www.sciencedirect.com
ScienceDirect
Journal of Power Sources 163 (2007) 952–956
JOURNAL OF POWER SOURCES
www.elsevier.com/locate/jpowsour

Short communication

Influence of annealing of membrane electrode assembly (MEA) on performance of direct methanol fuel cell (DMFC)

Ho-Young Jung [a], Ki-Yun Cho [a], Yong Min Lee [a], Jung-Ki Park [a,*], Jong-Ho Choi [b], Yung-Eun Sung [c]

[a] *Department of Chemical and Biomolecular Engineering, Korea Advanced Institute of Science and Technology, 373-1, Guseong-dong, Yuseong-gu, Daejeon 305-701, Republic of Korea*
[b] *Department of Materials Science & Engineering, Gwangju Institute of Science and Technology, Gwangju 500-712, Republic of Korea*
[c] *School of Chemical Engineering, Seoul National University, Seoul 151-742, Republic of Korea*

Received 14 June 2006; received in revised form 12 August 2006; accepted 15 September 2006
Available online 13 November 2006

Abstract

The influence of annealing of membrane electrode assembly (MEA) of a direct methanol fuel cell (DMFC) on the cell performance was investigated. The annealing was conducted at various temperatures of 110, 130, 150 and 200 °C. Annealing at 130 °C could produce highest proton conductivity of the recast Nafion binder and electrochemical active surface area of the electrode, leading to the highest cell performance.

Keywords: Direct methanol fuel cell; Binder; Annealing; Recast Nafion film

1. Introduction

Nafion has been typically used as a polymer electrolyte membrane and also as an electrode binder in direct methanol fuel cell (DMFC) owing to its advantages such as high proton conductivity and good chemical stability. Commercially, different grade of Nafions are produced and the recast Nafion is commonly considered for binder of the electrode of DMFC, while Nafion membranes including Nafion 117 are used for the electrolyte membrane of the cell.

Polymer binder plays an important role in the operation of fuel cell by keeping the integrity of the electrode and also providing the proper phase for migration of protons in the electrode. It was already reported that the recast Nafion, which can be a binder of the electrode, is dissolved in ethanol solution and the dissolution is much prevented by annealing of the binder film [1,2]. This result brought us the idea that annealing of membrane electrode assembly (MEA) rather than the binder itself could influence the microstructure of the electrode and the consequent cell performance.

In this work, the annealing of MEA was performed at various temperatures, especially below and above the glass transition temperature of the recast Nafion binder and structural and electrochemical characteristics of the resulting electrode and also the cell performance were evaluated.

2. Experimental

2.1. Preparation of MEA

The electrodes were prepared by using a brushing technique to coat the catalytic layer on carbon paper (TGPH090, Toray). Pt catalyst (5 mg cm^{-2}) and Pt/Ru catalyst (5 mg cm^{-2}) were applied to the cathode and the anode, respectively. The MEAs were prepared by hot-pressing the electrodes onto a Nafion 117 membrane and additionally annealed at various temperatures of 110, 130, 150 and 200 °C for 40 min. This additional longer annealing to the hot-pressing process was introduced to produce the favorable change in morphology of the electrode for

* Corresponding author. Tel.: +82 42 869 3965; fax: +82 42 869 3910.
E-mail address: jungpark@kaist.ac.kr (J.-K. Park).

0378-7753/$ – see front matter © 2006 Elsevier B.V. All rights reserved.
doi:10.1016/j.jpowsour.2006.09.047

higher performance of MEA. The performances of MEA were evaluated by using the 2 cm^2 single cell.

2.2. Dissolution measurement of the recast Nafion binder

Nafion suspension (5 wt.%) was procured from Du Pont. The Nafion binder films were prepared by casting the Nafion suspension onto a Pyrex petri dish and slow evaporation of the solvent at 70 °C. These recast films were soaked in water bath and then peeled off.

Dissolution of the recast Nafion binder films was evaluated in accordance with the procedures published elsewhere [3]. Experimental procedures were as follows; the recast Nafion binder films were dried for 1 h in a vacuum oven at 80 °C. Dried binder films were weighed and sonicated in a methanol/water mixture (2 M) for 24 h. Solid residues were then filtered out and dried in a vacuum oven for weighing measurement. The dissolution is determined in weight percentage, calculated from the ratio of the final weight divided by the initial weight of the film.

2.3. DSC measurement

Differential scanning calorimetry (DSC) measurements were carried out by using a TA Instruments DSC 2010 in a nitrogen atmosphere at a temperature range of −50 to 300 °C, with a heating rate of 10 °C min^{-1}.

2.4. Impedance spectroscopic measurement

The proton conductivities were determined by using an ac impedance spectroscopy. The impedance spectroscopy instrument was composed of a Solartron Instruments 1287 electrochemical interface and a Solartron Instruments 1255 impedance phase analyzer, both of which were interfaced via GPIB to a computer. The electrochemical impedance spectra were recorded over a frequency range of 1 Hz–1 MHz, the amplitude of the sinusoidal modulation voltage was 10 mV. A membrane of 1.5 cm in diameter was placed between two stainless steel (STS) disk electrodes of the same diameter. All conductivity measurements were performed with the film at its fully hydrated state.

The impedance experiment for the DMFC was carried out at 0.4 V; the ac amplitude was 10 mV and the frequency was typically varied from 0.05 to 5000 Hz and the cell was operated at 30 °C; the flow rate of oxygen and methanol solution (2 M) were maintained at 200 and 1 cm^3 min^{-1}, respectively.

2.5. Water uptake measurement

All the samples were dried in a vacuum oven at 80 °C for 3 days before water uptake measurements. Then the samples were immersed and maintained in deionized water for 3 days at 25 °C to attain equilibrium water uptake. The water uptake was determined as follows:

$$\text{Water uptake}\,(\%) = \frac{W_s - W_d}{W_d} \times 100 \quad (1)$$

where W_s and W_d are the weights of swollen and dried samples, respectively. The weights of the swollen films were measured immediately after carefully removing the water from both surfaces [4].

2.6. X-ray diffraction experiment

Wide-angle X-ray diffraction data were obtained on a Rigaku D/max-rc (12 kW) wide-angle thin film diffractometer equipped with a rotating Cu anode and a monochromator in a scanned region of 10° and 20° (2θ).

Small-angle X-ray scattering (SAXS) experiments were also performed using a Bruker small-angle X-ray with general area detector diffraction system (GADDS) equipped with a Cu Kα radiation generator (3 kW), a two-dimensional detector (Hi-Star) and a goniometer. The distance between the film and the detector was set at 300 mm. All of the scans were normalized in accordance with the procedure described elsewhere [5].

2.7. Morphology characterization

Pore volume distribution measurements for the electrodes were conducted using a BET surface analyzer. The morphology of the electrode was examined by means of a field emission SEM equipped with a high-resolution secondary electron detector.

2.8. Cyclic voltammetry (CV)

Cyclic voltammetry measurements were performed at 30 °C on 2 cm^2 geometric area single cell fixtures to determine the electrochemical active surface area. The measurements were based on hydrogen and nitrogen at the counter electrode (anode) and working electrode (cathode), respectively, with a potential range of 0.01–1.2 V versus RHE maintaining a sweep rate of 10 mV s^{-1}. The electrochemical active surface area of the electrode was obtained from the charge required for hydrogen desorption from the Pt electrocatalyst. The coloumbic charge for the oxidation of atomic hydrogen was used to evaluate the roughness factor of the electrode assuming a value of 210 μC cm^{-2} for the oxidation of atomic hydrogen on smooth Pt surface.

3. Results and discussion

According to the previous method reported previously for dissolution examination of the recast Nafion in ethanol solution, we investigated dissolution of the recast Nafion (recast from Nafion dispersion of Du Pont) in aqueous methanol solution, the most common fuel in the anode side of DMFC, with annealing.

Fig. 1 shows the effect of annealing temperature of the recast Nafion on dissolution in methanol solution. It can be seen that dissolution of the recast Nafion strongly depends on the annealing temperature. Above T_g of the recast Nafion (130 °C), with increase of the annealing temperature, the dissolution is found to decrease very significantly. This is because with annealing there is a change in morphology of the recast Nafion.

It has been already reported that the crystalline state is developed with annealing of the Nafion [6,7]. The increase of crys-

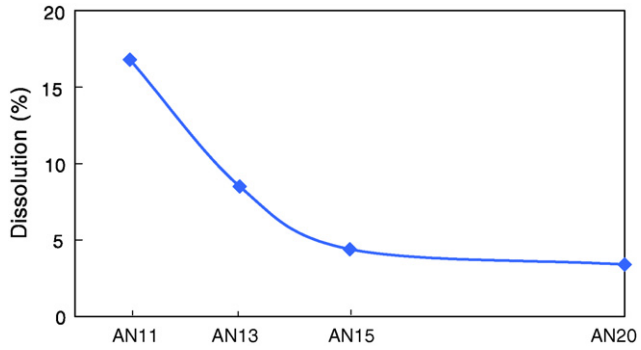

Fig. 1. The dissolution of annealed recast Nafion films in aqueous methanol fuel. The films were annealed for 40 min at different temperatures of 110, 130, 150 and 200 °C and are denoted as AN11, AN13, AN15 and AN20, respectively.

tallinity of our recast Nafion with annealing is well presented in X-ray diffraction spectra shown in Fig. 2. The increase of crystallinity of the recast Nafion with annealing can explain that the dissolution of Nafion binder is much suppressed with annealing since the crystalline structure is much more resistant to dissolution due to their higher chain packing density [3]. It is noted from our experiment (the data not shown) that the Nafion 117 membrane is not dissolved at all in methanol/water mixture (2 M) even after sonication for 1 day. This is due to its higher crystallinity compared with that of the recast Nafion [3].

Proton conduction of the recast Nafion is also of high importance to the performance of the electrode and also the fuel cell. The annealing will also influence proton conductivity of the recast Nafion film. Fig. 3 represents proton conductivity changes with annealing of the recast Nafion. The annealing was performed in the temperature range between 110 and 200 °C. It is interestingly found that proton conductivity is highest (5.5×10^{-3} S cm^{-1}) around 130 °C.

Proton conduction is mainly influenced by water uptake of the membrane when the proton sources are same. As shown in Fig. 4, the water uptake is most prominent at the annealing temperature of 130 °C, which is consistent with the proton conduction behavior. The highest uptake at 130 °C is associated with morphology of the recast Nafion.

Fig. 5 shows small angle X-ray scattering spectra for the annealed recast Nafion film. The firstly appearing scattering peak

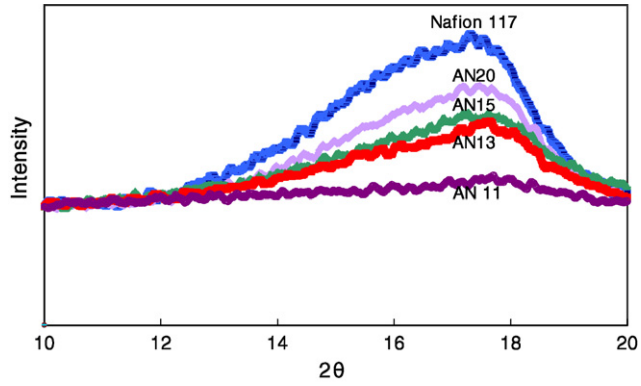

Fig. 2. WAXD profiles of Nafion 117 membrane and annealed recast Nafion films.

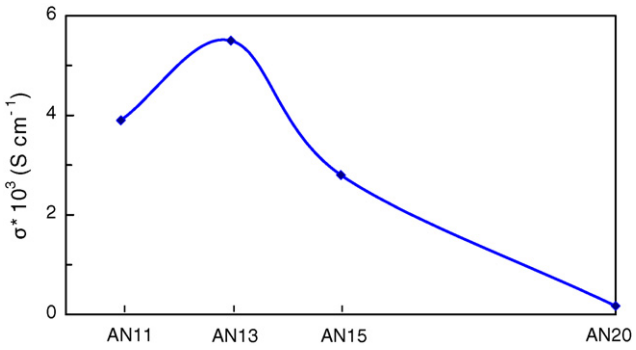

Fig. 3. The proton conductivities of annealed recast Nafion films.

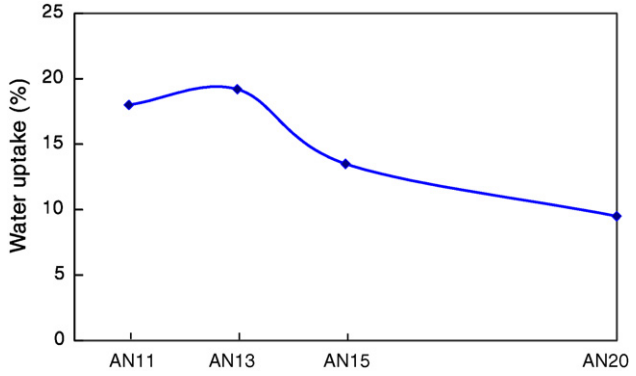

Fig. 4. The water uptake of annealed recast Nafion films at 25 °C.

($s \approx 0.1$ nm^{-1}) is attributed to the scattering by crystalline region and the second peak ($s \approx 0.35$ nm^{-1}) originates from the presence of ionic clusters [6]. The intensity of the second peak is highest for the film annealed at 130 °C, indicating that the ionic clusters in the film is most efficiently produced at 130 °C. During annealing, both the crystalline structures and the ionic clusters in the film may be developed. Chain mobility is considered to play an important role in formation of ionic clusters. The enhanced chain mobility with increase in temperature especially above the glass transition temperature, 130 °C, would help formation of the ionic clusters, however, development of the crystalline in the film is also enhanced. This crystalline development can

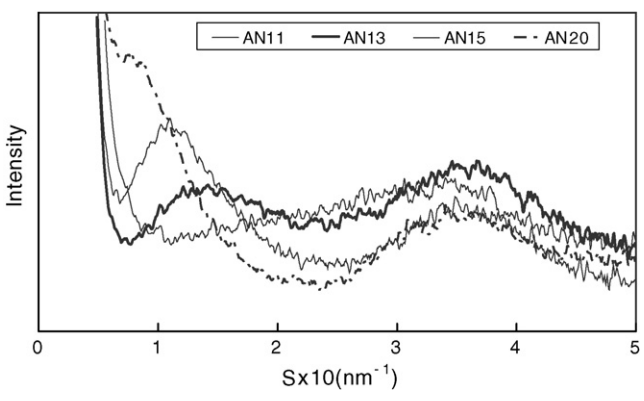

Fig. 5. SAXS profiles of recast Nafion films.

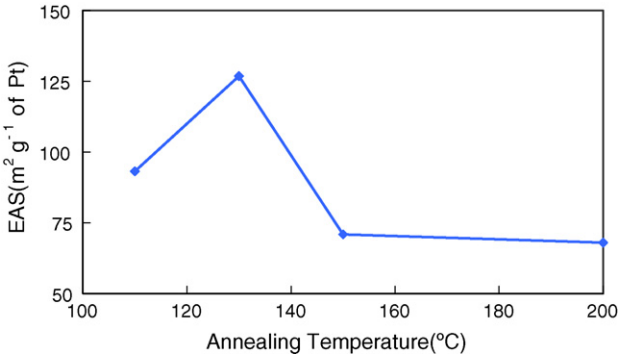

Fig. 6. Electrochemical active surface areas of the electrodes as a function of annealing temperature.

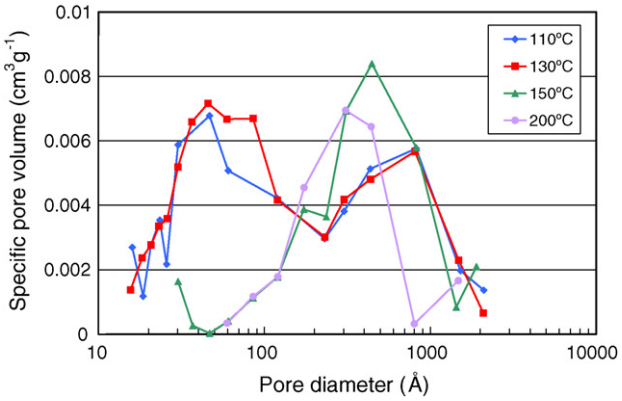

Fig. 7. The pore size distributions of the electrode as a function of annealing temperature.

reduce chain mobility and thus there should be a proper annealing temperature for efficient ionic cluster formation.

The electrochemical active surface (EAS) is the effective surface area of the platinum in the electrode for electrochemical reaction. For the EAS measurements, the electrode specimens were prepared separately from MEA and annealed for 40 min at various temperatures of 110, 130, 150 and 200 °C. Fig. 6 shows the change of the EAS with annealing temperature and the highest EAS is observed for the electrode annealed at 130 °C. The EAS would be influenced by the pore-size distributions in the electrode [8]. Fig. 7 presents pore-size distributions with change of annealing temperature of the electrode and they exhibit two distinctive modes, with the primary pores between 30 and 100 Å which are presumably associated with the free space near the electrocatalyst surface and the secondary ones between 300 and 800 Å. From the change in distribution of pore size with annealing temperature, it is expected that at higher annealing temperatures of 150 and 200 °C, the primary pores are readily blocked, while the size of the secondary pores is increased. The primary pores are most abundant at the annealing temperature of 130 °C, which seems to importantly influence on the cell performance. The fact that the primary pores are easily blocked at rather higher temperatures might be associated with the higher chain mobility of the binder and the consequent diffusion of the chains to the primary pores. The more favorable diffusion of the chains of the binder to the primary pores rather than to the secondary pores would be due to much larger number of the available primary pores compared to that of secondary pores.

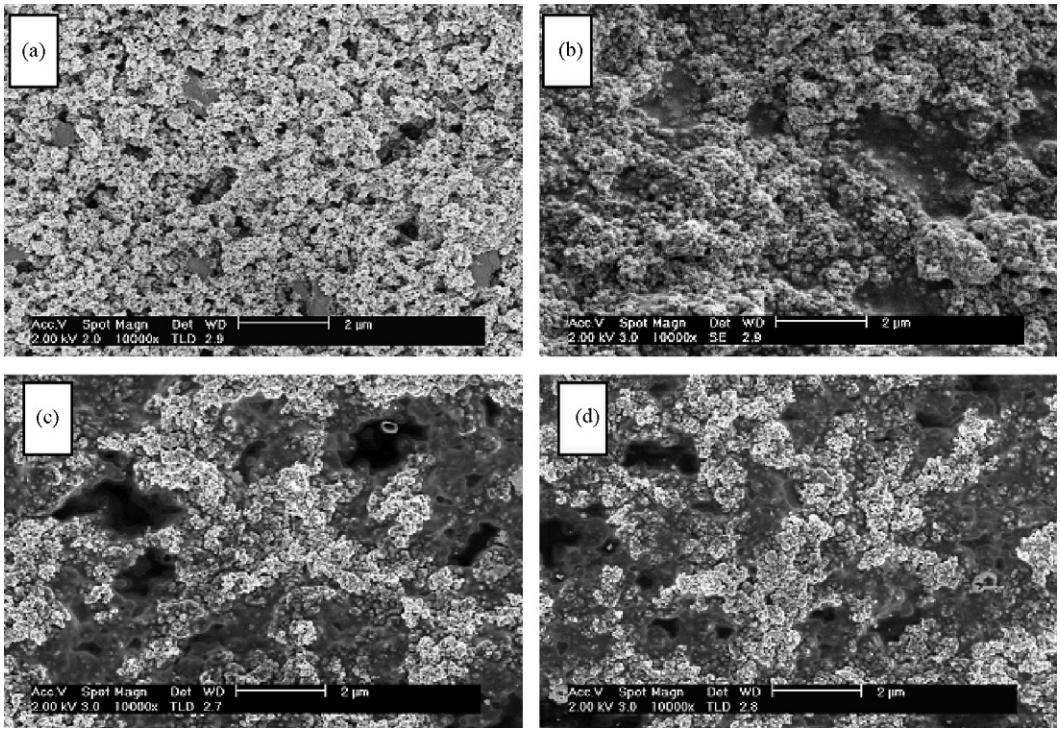

Fig. 8. SEM photographs of surface of the catalyst layer for electrode annealed at: (a) 130 °C, (b) 110 °C, (c) 150 °C and (d) 200 °C.

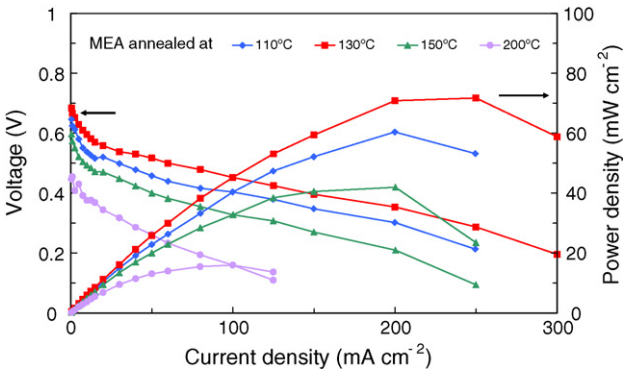

Fig. 9. Polarization curves of the cells based on MEA annealed at different temperatures ($C_{MeOH} = 2$ M, $f_{MeOH} = 1\ cm^3\ min^{-1}$, $f_{O_2} = 200\ cm^3\ min^{-1}$, $T_{cell} = 30\,^{\circ}C$).

The above changes of pore distributions with the annealing temperature are well observed from SEM images of the electrode. Fig. 8 shows the SEM images of the electrode surfaces annealed at different temperatures. From Fig. 8(a) representing the surface image of the electrode annealed at 110 °C quite lower than the T_g of recast Nafion, it is observed that the recast Nafion chains are in aggregates. These aggregates become loose and spread out at the annealing temperature of 130 °C as is exhibited in Fig. 8(b). For the higher annealing temperatures of 150 and 200 °C, as shown in Fig. 8(c and d), the catalyst particles are increasingly covered with the recast Nafion chains and the primary pores become blocked.

Fig. 9 shows polarization curves of the cells constructed with MEA's annealed at various temperatures. The cell performance was tested at 30 °C after 3 days operation. The cell based on MEA annealed at 130 °C shows the highest performance as is expected from the above considerations.

4. Conclusion

The effect of annealing of MEA containing the recast Nafion as a binder on the performance of DMFC was investigated. Annealing at 130 °C, which is around glass transition temperature of the recast Nafion binder, could provide the highest proton conductivity of the recast Nafion binder in the electrode. This could be explained in terms of ionic cluster behavior of the binder film. For electrodes, the electrochemical active surface area was also highest at the annealing temperature of 130 °C. It seems to be associated with the available number of the primary pores in the electrode. These could lead to a highest performance of the cell at 130 °C. It is strongly proposed that annealing of MEA is one of the useful means of enhancing the cell performance.

Acknowledgements

This work is supported by the Core Technology Development Program for Fuel Cell of Ministry of Science and Technology and Korea Institute of Energy Research Evaluation and Planning.

References

[1] L.A. Zook, J. Leddy, Anal. Chem. 68 (1996) 3793.
[2] Z. Siroma, N. Fujiwara, T. Ioroi, S. Yamazaki, K. Yasuda, Y. Miyazaki, J. Power Sources 126 (2004) 41.
[3] R.B. Moore III, C.R. Martin, Macromolecules 21 (1988) 1334.
[4] M.D. Kurkuri, T.M. Aminabhavi, J. Controlled Release 96 (2004) 9.
[5] T.D. Gierke, G.E. Munn, F.C. Wilson, J. Polym. Sci. Polym. Phys. 19 (1981) 1687.
[6] M. Fujimura, T. Hashimoto, H. Kawai, Macromolecules 14 (1981) 1309.
[7] G. Gebel, P. Aldebert, M. Pineri, Macromolecules 20 (1987) 1425.
[8] E. Antolini, L. Giorgi, A. Pozio, E. Passalacqua, J. Power Sources 77 (1999) 136.